



Contents lists available at ScienceDirect

Analytica Chimica Acta

journal homepage: www.elsevier.com/locate/aca

Correction of self-absorption effect in calibration-free laser-induced breakdown spectroscopy (CF-LIBS) with blackbody radiation reference

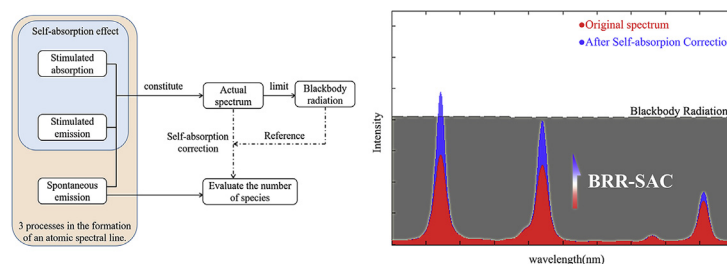
Tianqi Li, Zongyu Hou, Yangting Fu, Jianlong Yu, Weilun Gu, Zhe Wang*

State Key Lab of Power System, Department of Energy and Power Engineering, Tsinghua-BP Clean Energy Centre, Tsinghua University, Beijing, 100084, China

HIGHLIGHTS

- A new self-absorption correction method based on black-body radiation reference was proposed.
- The proposed method applied all the spectral lines and does not need the stark broadening coefficient.
- Experimental results proved that both the linearity of the Boltzmann plot and the measurement accuracy was improved.
- The proposed method has additional uses and expanded potential.

GRAPHICAL ABSTRACT



ARTICLE INFO

Article history:

Received 5 November 2018
 Received in revised form
 3 December 2018
 Accepted 14 January 2019
 Available online xxx

Keywords:

Laser-induced breakdown spectroscopy
 Self-absorption
 Blackbody radiation
 Calibration-free quantitative analysis
 Boltzmann plot

ABSTRACT

The self-absorption effect due to optically thick property greatly influences the measured line intensities as well as the performance of quantification for laser-induced breakdown spectroscopy (LIBS) especially for calibration-free LIBS which requires proper correction. In this paper, a new self-absorption correction method for Calibration-Free LIBS (CF-LIBS), called *blackbody radiation referenced self-absorption correction* (BRR-SAC) is proposed. An iterative algorithm was designed to calculate the plasma temperature and normally hard-to-obtain collection efficiency of the optical collection system by directly comparing the measured spectrum with the corresponding theoretical blackbody radiation for self-absorption correction. Compared with generally applied self-absorption correction methods based on the principle of curve of growth, the proposed method has obvious advantages of simpler programming, higher computation efficiency, and its independency of the availability or accuracy of line broadening coefficients. Experiments were conducted on titanium alloy samples. The experimental results showed that the self-absorption was corrected with increased linearity of the Boltzmann plots and the measurement accuracy of the elemental concentration was significantly improved through BRR-SAC. Compared with the traditional CF-LIBS with self-absorption correction, the proposed method also showed better performance. In addition, BRR-SAC provides a simple way to obtain the collection efficiency of the experimental setup, which benefits the plasma diagnostics and quantitative analysis.

© 2019 Elsevier B.V. All rights reserved.

1. Introduction

Laser-induced breakdown spectroscopy (LIBS) has been regarded as the most versatile technique for elemental analysis and has shown great potentials in many applications [1–3]. Calibration methods [4–9] generally provide good quantitative results and

* Corresponding author.

E-mail address: zhewang@tsinghua.edu.cn (Z. Wang).

therefore are more commonly applied. However, these methods require a set of calibration sample with certified elemental concentration, which may be not available for some conditions. In comparison, calibration free method provides a unique advantage. Since Ciucci et al. [10] introduced the calibration-free LIBS, in which Boltzmann plots relied on local thermodynamic equilibrium (LTE) assumption. CF-LIBS has been widely applied in quantitative analysis for alloys [11–22], glasses [23], pigments [24], soils and rocks [25–27], even aerosols [28]. However, some assumptions made in CF-LIBS have reduced its accuracy [29], for example, LTE, stoichiometric ablation, optically thin and homogeneous plasma. In this work, we mainly focus on reducing the self-absorption effects resulting from the optically thick property under the context of CF-LIBS method.

Originally, CF-LIBS was based on optically thin assumptions, meaning no self-absorption. Besides, Boltzmann plots was utilized to estimate the plasma temperature and to determine the species concentration in a sample. However, plasma is usually not optically thin, and therefore the presence of self-absorption reduces line intensities and degrades Boltzmann plots [30], leading to larger measurement errors for calibration-free method. Self-absorption occurs when plasma light is re-absorbed by the same kind of elements which emitted the light along the optical length, thereby flattening the line profile or in extreme cases generating a dip in the line center (called self-reversal) [31]. Various methods have been developed to deal with this problem. The first category of self-absorption correction methods was based on the principle of curve of growth (COG). Bulajic et al. [16] used COG for self-absorption correction, in which the effect of self-absorption on line profile was clarified and an iterative algorithm was proposed to calculate plasma temperature, electron number density, Gaussian broadening, Lorentzian broadening, and optical path length. However, this method has high complexity due to the excessive iteration variables. Based on Bulajic's method, Praher et al. [32] investigated the relationship between line broadening and self-absorption extent, and proposed a simplified iterative algorithm. For this methods and others [33–35], there are inevitable uncertainties in the estimation of electron density from Stark broadening, which will greatly affect the performance of self-absorption correction and increase the algorithm complexity. In addition, for many lines, their Stark broadening coefficients may be very difficult to obtain, which limits the application of these methods. Another category of self-absorption correction methods was based on the selection of internal reference line intensity. Sun et al. [15] proposed an internal reference for self-absorption correction (IRSAC) method with one or several lines as internal reference, which was regarded as free from self-absorption. In Sun's method, the intensity of other lines was calculated by the reference line intensity and estimated plasma temperature based on theoretical equation. The IRSAC method is very easy to employ and computationally efficient, but the method only retains the internal reference line intensities and all other measured line intensities actually are not significant for the final plasma temperature estimation as well as concentration calculation. Therefore, the IRSAC method lacks the solid physical principle and is not applicable for those cases without appropriate internal references. For the methods based on IRSAC, such as the internal reference–external standard with the iteration correction (IRESIC) procedure proposed by Dong et al. [36], in which one standard sample matrix-matched along with the genetic algorithm (GA) was utilized to estimate the plasma temperature, the same disadvantages remain. In addition to these two mainstream methods, some other methods have also been proposed. Demidov et al. [37] proposed an improved Monte-Carlo (MC) method for standard-less analysis, where the concentrations in LIBS were found by fitting model-generated synthetic spectra to

experimental spectra. Since this method requires a great amount of computational resource, it is not suitable for many scenarios. Moon et al. [38] proposed a method for selecting spectral lines with self-absorption by comparing spectra acquired with and without a duplicating spherical mirror placed behind the plasma plume. This method has additional requirements for the experimental device, which limits its application especial to harsh conditions. Recently, Zhu et al. [39] proposed an approach to overcome the self-absorption effect using molecular emission. However, this method is not widely applicable for the conditions without molecular emission.

In this work, a new self-absorption correction method called *blackbody radiation referenced self-absorption correction* (BRR-SAC) was proposed by taking collection efficiency and plasma temperature as two unknowns in the integration process in CF-LIBS. Based on the relationship between blackbody radiation and self-absorption, an iteration algorithm was designed to calculate the two parameters and elemental concentrations. Compared with COG-based self-absorption method, the proposed BRR-SAC method shares the same physical background, and has the obvious advantages of simpler programming, higher computation efficiency, and its independency of the calculation of electron density and Stark broadening. Compared with internal reference based method, BRR-SAC is more robust since it fully utilizes all measured line information and contains the COG physical background. Experiments were also performed on titanium alloy samples and the results verified the effectiveness of the BRR-SAC method. Further merits of this method include the explicit calculation of the number density of species in plasma and collection efficiency.

2. Methods

The relationship between blackbody radiation and self-absorption has been extensively investigated [40,41]. However, since plasma temperature and collection efficiency are not available in many cases, the experimental spectrum and blackbody radiation cannot be directly compared. In this paper, an iterative process was designed to continuously assign and correct these two parameters and finally achieve self-absorption correction. The process of this method is as follows. Firstly, the relationship between blackbody radiation and self-absorption determines that, the degree of self-absorption depends on the ratio of line intensity to blackbody radiation intensity that depends on the plasma temperature and collection efficiency. Therefore, these two parameters will affect the corrected spectral line intensity. Then the Boltzmann plot describes the relationship between the intensities of the corrected spectral lines and determines the plasma temperature. Therefore, the actual collection efficiency and plasma temperature can make the Boltzmann plot have the best linearity and conform to the Boltzmann plot's description of the plasma temperature.

In this section, the relationship between blackbody and self-absorption will be briefly described. According to the phenomenology by Einstein, there are three processes in the formation of an atomic spectral line, i.e. spontaneous emission, stimulated emission, and stimulated absorption. On the one hand, for the plasma in LTE, stimulated emission and stimulated absorption collectively show the self-absorption effect which can reduce the emission intensity and the reduction is proportional to the emission intensity itself. On the other hand, the amount of spontaneous emission can characterize the number of species according to the Boltzmann equation. Therefore, without considering the spatiotemporal inhomogeneity, the ultimate goal of self-absorption correction is to eliminate the effects of stimulated emission and stimulated absorption on the spectrum and extract the spontaneous emission from the spectrum.

In many LIBS experiments, the light collected by fiber mainly comes from the part of plasma that is very close to the optical axis of this collecting lens. This means the plasma can be considered as a 1-D strip if we ignore the part that has no effect on the spectrum [43]. In this case, the intensity of radiation $I(\lambda)$ from the homogeneous plasma strip (length l) can be expressed as [38].

$$I(\lambda) = F \cdot L_P(\lambda) \cdot [1 - \exp(-\tau(\lambda))], \quad (1)$$

where F is the coefficient of collection that considers the optical efficiency of the collection system as well as the transverse area of the region of the plasma, $L_P(\lambda)$ is the blackbody radiation and $\tau(\lambda)$ is the optical length.

Eq. (1) shows the expression of the spectral intensity that is obtained experimentally, and it can be understood as follows: when the optical path of the plasma is infinitely thick, its radiation intensity tends to be blackbody radiation intensity rather than infinitely large because of strong self-absorption.

Besides, the expression of the intensity of spontaneous emission I^* (i.e, the intensity after self-absorption correction) is given by:

$$I^*(\lambda) = F \cdot L_P(\lambda) \cdot \tau(\lambda) \quad (2)$$

It can be seen from Eq. (2) that when $\tau(\lambda)$ is very small, $\tau(\lambda) \approx 1 - \exp(-\tau(\lambda))$, and the self-absorption effects can be ignored under this condition. For the traditional CF-LIBS method, according to the optical thin assumptions, the experimentally measured I is considered to be equal to I^* and the Boltzmann plot is drawn based on I . However, $I^*(\lambda)$ will be larger than $I(\lambda)$ when $\tau(\lambda)$ is not too small, under which condition the error of measurement will become larger if the correction is not performed.

We found the optical length $\tau(\lambda)$ can be obtained by comparing the plasma spectrum $I(\lambda)$ with blackbody radiation intensity corresponding to the spectrum $F \cdot L_P(\lambda)$ and then the line intensity after self-absorption correction can be obtained. Since there are only two unknown variables, i.e. coefficient of collection F and plasma temperature T , the calculation results of the corrected line intensity are affected by the values of F and T . Besides, since Boltzmann plot describes the relationship among the intensities of the corrected spectral lines and also determines the plasma temperature, it is considered to be the key tool for determining the F and T . More specifically, the actual F and T can not only make the Boltzmann plot has the best linearity, but also consistent with the temperature described by the Boltzmann plot. In order to determine the values of T and F , we design the following iterative algorithm and self-absorption correction method:

Firstly, the F and T are assigned with the initial values. Blackbody radiation intensity L_P is calculated according to T , and the corrected intensity I^* is calculated based on F , L_P and I . Secondly, the linearity of the Boltzmann plot based on I^* is evaluated using the least squares criterion method, with the main evaluation parameter as the correlation coefficient (r [2]). For a particular T , there will be a specific F maximizes the correlation coefficient. The plasma temperature described by the Boltzmann plot is recorded as T' . If T' is not equal to the initial temperature T , then modify the initial value of T until these two are equal. Finally, the content of each element in the sample are calculated according to the final Boltzmann plot. The flow chart of the BRR-SAC method is shown in Fig. 1.

More details of the iterative process are described as follows: 1) the initial value of the collection coefficient F and the temperature T are empirically selected, which has little effect on the final results. For example, the value of F is about 10^{-9} and the T is about 1eV. 2) In Eqs. (1) and (2), I and I^* refers to the power density in the spectrum. Therefore, for a particular line, its intensity needs to integrate the spectrum over a certain range. Fortunately, the self-

absorption effect does not change this range, which saves a lot of computational resource. 3) The linearity of the Boltzmann plot is characterized by correlation coefficient (r [2]), which can be understood as a function of F , but its expression is very complicated. As F decreases, the difference between I and I^* becomes more remarkable, which is reflected in the larger upward movement on the Boltzmann plot. Therefore, r [2] will increase first and then decrease until F is too small to solve I^* . 4) Empirical practice shows that if the T' is assigned to T , the iteration process can converge very quickly, so as to reduce the computational resource in the entire iteration process.

The highlight of the BRR-SAC method is that the plasma spectrum is directly compared with blackbody radiation and the self-absorption is used as a tool to obtain the key parameter F . Although F can be estimated by geometrical optics under simple experimental condition, but it is not available when the light-collecting system is complicated or the experimental plasmas obviously changes. In addition, the collection coefficient and blackbody radiation are indispensable for plasma diagnostics. For example, Hermann et al. [42] evidenced the local thermodynamic equilibrium in a laser-induced plasma by blackbody radiation.

The above description has shown that the BRR-SAC method can achieve the self-absorption correction simply and quickly by reasonably selecting iterative variables. Compared with the COG method, BRR-SAC requires less computational resource, and is easier to program. Compared with IRSAC, BRR-SAC makes full use of experimental data and has greater robustness. Compared with the method based on line broadening, BRR-SAC does not rely on the acquisition of electron density and Stark broadening.

BRR-SAC is especially suitable for the samples with many spectral lines such as steel and titanium alloy. For those samples with few spectral lines, we can first obtain the F by the experiments with other samples and then correct the self-absorption.

3. Experimental

A standard LIBS setup was used in this experiment. The laser beam from the Q-switched Nd: YAG laser (Q-Smart 100, Quantel, France), operating at wavelength of 1064 nm with an energy of 80 mJ, a pulse duration of 4 ns, and a repetition rate of 1 Hz, was used to generate plasma on the sample surface. The focusing was kept inside the sample surface to avoid air ignition and to minimize air interference on the emission spectra. The spot size at the focus was approx. 0.2 mm. The emission of laser-induced plasma was collected using an achromatic silica lens. The light was guided by a quartz fiber into an Echelle spectrometer with intensified CCD detector (Aryelle Butterfly, LTB, Germany) employing delay time of 1 μ s, 2 μ s and 3 μ s with respect to the laser pulse and a gate time of 0.05 μ s. The fiber used in the experiment had a diameter of 400 μ m and a numerical aperture of 0.224. The delay time was sufficient to suppress the background signals from continuum plasma radiation. A short gate time was chosen to avoid large changes in plasma temperature and electron number density during the measurement. The wavelength of recorded spectra range was from 180 nm to 430 nm with a spectral resolution of $\lambda/\Delta\lambda \geq 20,000$. A standard light source (DH-3plus, Ocean Tec, USA) was used for the intensity standardization of the optical fiber and spectrometer. The spectrum was accumulated by 10 laser pulse signals in order to improve the signal-to-noise ratio.

The samples used in the experiments were two standard titanium alloys (TC4, Chinese National Standard No.02503&02505) with known concentration. The alloy consisted of titanium, vanadium, aluminum and traces of iron, silicon and carbon.

In addition, the signal function measured by an optical spectrometer was obtained by the convolution of the "true" signal and

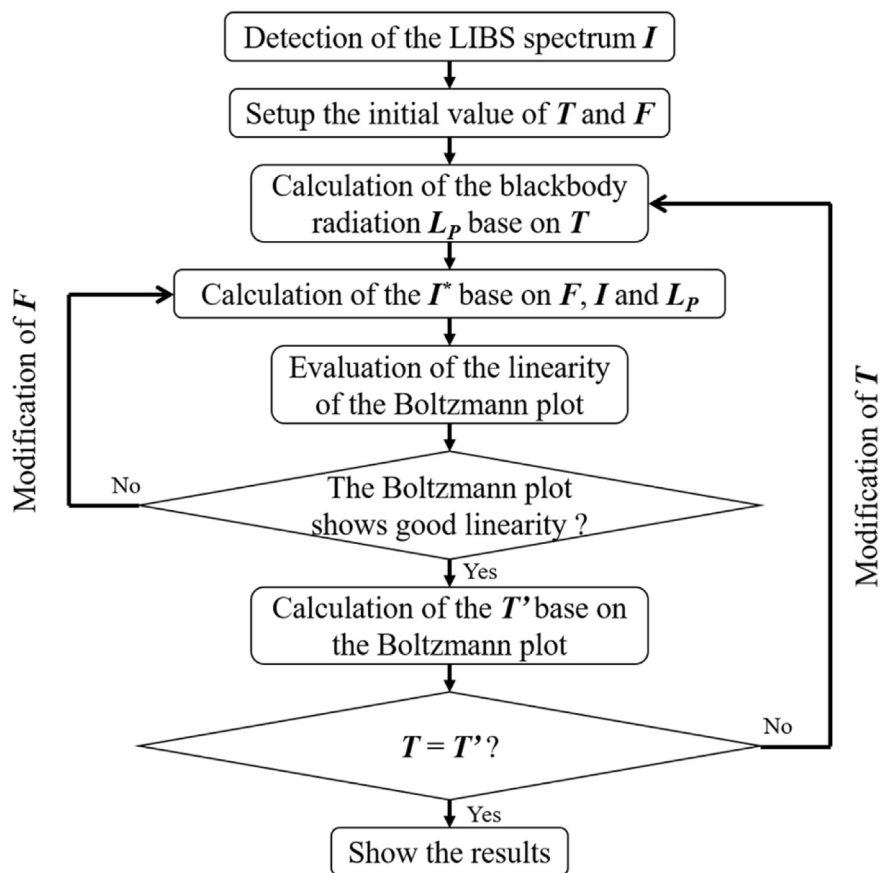


Fig. 1. The flow chart of the BRR-SAC method.

the transmission function of the spectrometer [32] and the true signal was derived by deconvolution using Richardson–Lucy method [44]. The deconvolution of the instrumental function can modify the peak intensity and the broadening of the spectral line, which is of great significance to the accuracy of the CF-LIBS method.

4. Results and discussion

4.1. Analytical lines selection

As titanium and vanadium element exist in the plasma mainly in the form of ions, a large number of titanium ion lines and vanadium ion lines can be found in the spectrum with high intensity. Many of them are accompanied by strong self-absorption, which is very advantageous to the study of the self-absorption effect correction. To improve the accuracy of the quantitative analysis results, the selected lines should meet the following conditions: 1) they should have strong enough intensity to ensure the signal-to-noise ratio, 2) their transition probability should have higher accuracy, and 3) they should not interfere with other lines. The selected lines are listed in Table 1 and their transition probabilities were obtained from the National Institute of Standards and Technology (NIST) database.

4.2. Boltzmann plots

Fig. 2 shows the Boltzmann plots, determined by the CF-LIBS without and with BRR-SAC method with different delay times. The left column (a, c, e) shows the Boltzmann plots before self-absorption correction while the right column (b, d, f) shows the

corrected results. The line of Ti II and V II are shown in the figure. Before the correction, the self-absorption lines make the points on Boltzmann plots in a very scattered pattern. Moreover, for the matrix elements, Ti, most of their analytical lines with high intensity exhibited strong self-absorption. The self-absorption effect caused higher calculated temperature than real values, lower intercepts, and finally large errors in the quantitative results. As shown in Fig. 2, The Ti II lines and V II lines show different slopes in Boltzmann plots.

After performing the correction using the proposed BRR-SAC method, the points on the Boltzmann plots show better linearity. In the correction process, two different cases happened for Ti II and V II. For V II, because their lines with low intensity were not affected by self-absorption, the correction process only slightly changed their line intensities, and the slopes and intercept of their fitting lines were nearly not changed. For Ti II, some lines were very strong and affected by self-absorption obviously. The correction process regulated those scattered points on the Boltzmann plots, and attained expected plasma temperatures and intercepts by these species themselves.

It can be seen from Fig. 2 that the effect of BRR-SAC under different experimental conditions (delay time) was similar: the linearity of titanium ions was significantly improved, while the linearity of vanadium particles changed little. The linearity of the Boltzmann plot was the optimal when the delay time was 2 μ s, which could be explained by the followings. When the delay time was too short, the broadening of the lines made them interfere with each other; when the delay time was too long, the interaction of the plasma with the surrounding environment made the plasma no

Table 1
The selected lines of Ti II and V II.

Species	Wavelength(nm)								
Ti II	251.743	252.560	252.975	253.125	253.462	253.587	257.103	283.218	
	284.193	285.110	286.232	287.743	288.410	301.718	302.973	304.668	
	305.974	307.522	307.864	308.803	309.718	310.380	310.508	310.623	
	311.205	311.980	315.225	315.419	315.567	316.852	319.087	320.253	
	321.705	321.827	322.284	322.424	323.228	324.198	324.860	325.291	
	325.294	325.425	328.233	330.880	331.532	331.802	332.170	332.293	
	332.676	332.945	333.211	333.519	333.785	334.376	334.674	336.618	
	336.920	339.457	340.242	340.720	340.981	345.246	345.638	346.555	
	347.718	349.105	350.489	351.084	352.025	353.541	357.373	358.713	
	359.605	365.976	366.223	370.622	374.164	390.054	391.346		
	V II	268.795	270.093	290.308	290.882	295.207	296.838	300.120	309.310
		310.230	311.071	313.333	313.494	313.652	326.770	351.730	354.520
	Ti I	395.633	395.820	398.176	398.975	399.863			
	Al I	394.400	396.152						

longer uniform. Subsequent calculations and discussions are mainly based on the case with the delay time of 2 μ s.

Fig. 3 shows the spectrum of the titanium alloy sample before and after self-absorption correction together with blackbody radiation. It can be found that for most of the spectral lines used for analysis, the optical lengths at their center wavelength are around 0.2–4. Besides, since there are no asymmetric or self-reversed patterns of any line in the spectrum, we believe that the plasma satisfies the assumption of uniformity.

4.3. Elemental concentration

Electron density is an important parameter in plasma. It can not only verify the accuracy of LTE, but also be used to calculate the number of other forms of species (such as Ti I, Ti III) of elements in plasma. The electron density can be calculated through the Saha-Boltzmann equation,

$$n_e = \frac{2(2\pi m_e kT)^{3/2}}{h^3} \frac{I_{mn}^l A_{ij} g_i^{II}}{I_{ij}^l A_{mn} g_m^I} \exp\left(-\frac{E_{ion} + E_i^{II} - E_m^I}{kT}\right), \quad (3)$$

where, m_e , k , T , and h are the mass of an electron, the Boltzmann constant, the temperature of the plasma, and the Planck's constant, respectively. I_{mn}^l , A_{mn} , g_m^I and E_m^I are the observed intensity of the line transition from m-level to n-level, the Einstein coefficient of the transition probability for spontaneous transition, the degeneracy of the upper level, and the energy of the upper energy level of an atomic line, respectively. Similarly, I_{ij} , A_{ij} , g_i^{II} and E_i^{II} are the corresponding parameters of an ionic line. E_{ion} is the 1st ionization energy.

A strong titanium atomic line (wavelength 395.82 nm) was selected for substitution into the Saha-Boltzmann equation. Different ionic lines were selected and the calculated electron density is averaged. The calculation result showed the electron density of the plasma was about $1.92 \times 10^{17} \text{ cm}^{-3}$.

In addition, we also tried to obtain the electron density by using the Stark broadening of Ti II 368.52 nm, the calculation result showed the electron density of the plasma was about $2.8 \times 10^{17} \text{ cm}^{-3}$. The difference might come from the self-absorption effect on the broadening of this line.

The number of the Ti III, V I, V III, Al II and Al III species can be calculated via Saha ionization equation,

$$\frac{n_{i+1}}{n_i} n_e = \frac{2(2\pi m_e kT)^{3/2}}{h^3} \frac{U_{i+1}}{U_i} \exp\left(-\frac{\varepsilon_i}{kT}\right), \quad (4)$$

where, n_i , U_i , and ε_i are the density of atoms in the i-th state of

ionization, the degeneracy of states for the i-ions and i-th ionization energy, respectively. Species with higher state of ionization were ignored and the final results are shown in Table 2, where the average error represents the average of the absolute values of the difference between the predicted concentration and the reference concentration of the three elements.

Table 2 also compares the results by the present work together with those by other methods. As can be seen from Table 2, BRR-SAC method shows the best results among all the listed methods. For traditional CF-LIBS method without self-absorption correction, the results are more deviated from the reference values than those with self-absorption correction, indicating the self-absorption effects; while for CF-LIBS with the IRSAC, its performance is heavily dependent on the selection of the reference line. It can be seen from Table 2 that the selection of different reference line (Ti II 310.50 nm or Ti II 325.29 nm) has led to quite different results. In addition, due to the unavailability of Stark broadening coefficient of the titanium ion line, we didn't use other self-absorption correction methods for comparison.

4.4. Coefficient of collection

Considering that the spectrometer and the fiber had been calibrated by standard light sources, coefficient of collection F actually represented the light collected efficiency multiplied by the effective collection area (m^2). Therefore, the value of F is deduced to be mainly affected by the experimental light collection system, and less affected by the plasma. In order to verify this conclusion, we collected the spectra under different delay time and calculated the value of F for the same sample (titanium alloy). In addition, for a light-collecting system without blocking and splitting, according to the principle of reversibility of light, its F can be expressed as a function of the fiber's numerical aperture NA and the diameter d :

$$F \approx \frac{1}{16} \pi d^2 NA^2, \quad (5)$$

It should be noted that the application of Eq. (5) has limitations: for example, the light-collecting lens should be large enough. According to the fiber parameters, the value of F in this experiment was about $1.58 \times 10^{-9} \text{ m}^2$ [2]. Table 3 shows that the experimental and reference values were very close in the early stage, which verified the reliability of the BRR-SAC method. It should be noted that as the delay time increased, the experimental and reference values were slightly deviated due to the possible failure in the hypotheses of uniformity and the local thermodynamic equilibrium.

The BRR-SAC method is able to obtain an accurate coefficient of

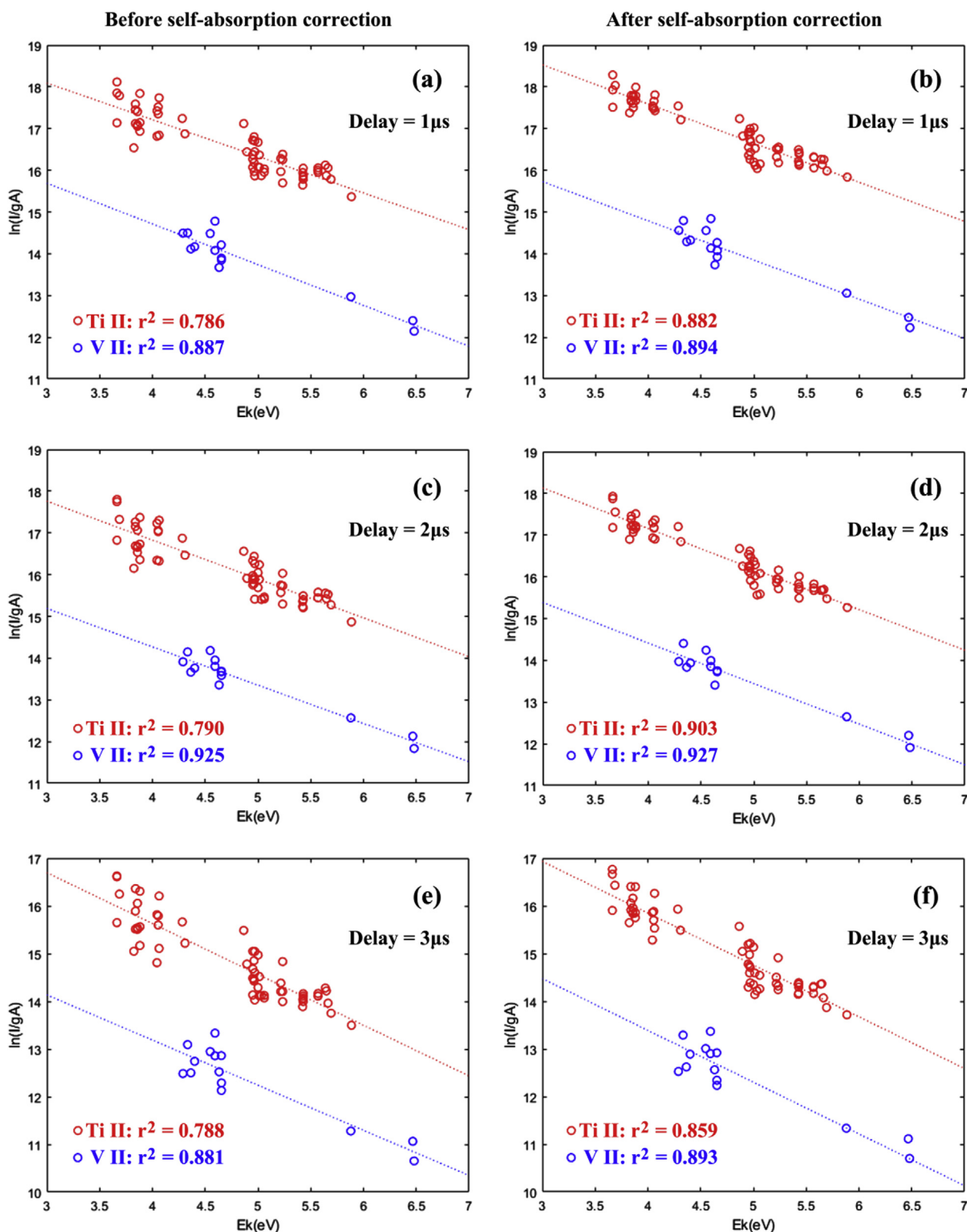


Fig. 2. The Boltzmann plots before and after self-absorption correction under different experimental conditions.

collection without any additional equipment, which is helpful for calculating the number density of various species in the plasma and is therefore significant for the quantitative analysis and mechanism analysis of LIBS. In this experiment, when the delay time was 2 μ s,

the number density of titanium ion (Ti II) was approximately $1.1 \times 10^{17} \text{ cm}^{-3}$ (the plasma length was estimated at 1 mm), which was a reasonable value.

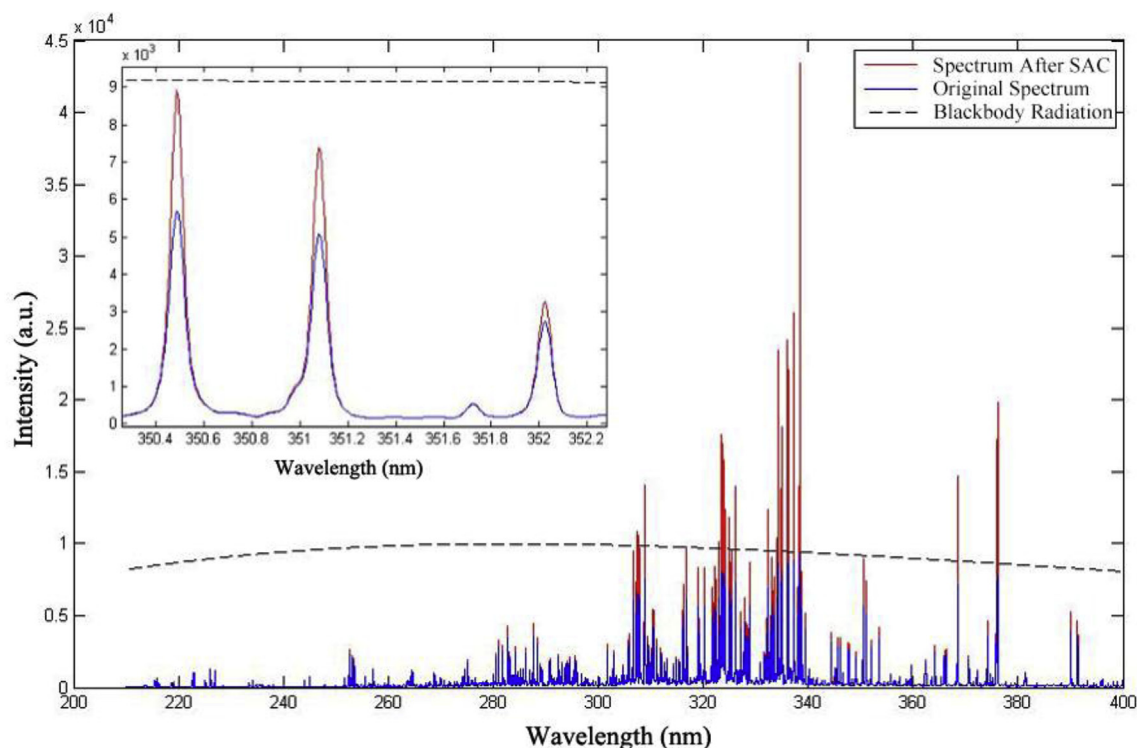


Fig. 3. The spectrum of the titanium alloy sample before and after self-absorption correction.

Table 2
Elemental concentration calculation results by different CF-LIBS methods.

Method		Elemental Concentration (wt%)			
		Ti (wt%)	V (wt%)	Al(wt%)	Average Error (wt%)
Sample 1	Traditional CF-LIBS	85.11	11.49	3.4	3.62
	CF-LIBS with IRSAC	87.57	8.93	3.5	1.91
	CF-LIBS with BRR-SAC	91.58	5.12	3.3	1.07
	Reference	90.05	5.9	4.05	0.27
Sample 2	Traditional CF-LIBS	88.12	6.76	5.12	2.08
	CF-LIBS with IRSAC	90.09	5.45	4.46	1.21
	CF-LIBS with BRR-SAC	90.67	3.44	5.89	0.21
	CF-LIBS with BRR-SAC	90.76	3.64	5.77	0.21
	Reference	90.76	3.41	5.38	/

^a The reference line is Ti II 310.50 nm.

^b The reference line is Ti II 325.29 nm.

Table 3
The coefficient of collection F calculated at different delay time.

Delay time	Coefficient of collection F	
	Sample 1	Sample 2
1 μ s	1.56×10^{-9}	1.56×10^{-9}
2 μ s	1.61×10^{-9}	1.54×10^{-9}
3 μ s	1.44×10^{-9}	1.47×10^{-9}
4 μ s	1.29×10^{-9}	1.35×10^{-9}
Reference	1.58×10^{-9}	

5. Conclusion

In laser-induced breakdown spectroscopy, the produced plasma is often optically thick. The research has shown that the higher the line intensity, the greater the self-absorption effect, which will usually lead to a relatively lower concentration. In order to correct

the self-absorption effect, we proposed a new method called BRR-SAC which used an iterative method to calculate the plasma temperature as well as the collection efficiency parameter by directly comparing the plasma spectrum and blackbody radiation intensity. The experimental results showed that, the Boltzmann plot achieved higher linearity, and quantitative analysis results were also greatly improved. Unlike other methods for self-absorption correction, BRR-SAC is able to make full use of the spectral lines and does not need the Stark broadening coefficient. BRR-SAC also provides a way to measure the efficiency of a light-collecting system without additional equipment, which is significant for the plasma diagnosis and quantitative analysis of LIBS.

In addition, BRR-SAC can be used as a pre-treatment method for calibration modeling rather than the usual combination with CF-LIBS. In our previous study, we proposed a dominant factor based partial least square (PLS) model [45–47], in which the dominant factor model was normally a univariate model and provided the

main information on concentration while PLS was employed for residual errors correction. It was found that the more accurate the dominant factor model, the better performance of the dominant factor based PLS method. It was also noticed that the dominant factor model was greatly influenced by self-absorption effect. Actually, BRR-SAC was originally designed for this purpose and the results will be present in future work.

Acknowledgements

The authors are grateful for the financial supports from National Natural Science Foundation of China (No. 61675110), National Key Research and Development Program of China (2016YFC0302102) and China State Key Lab. of Power System (SKLD17M12).

References

- [1] David A. Cremers, Rosemarie C. Chinni, Laser-induced breakdown spectroscopy—capabilities and limitations, *Appl. Spectrosc. Rev.* 44 (6) (2009) 457–506.
- [2] Z. Wang, T.B. Yuan, Z.Y. Hou, W.D. Zhou, J.D. Lu, H.B. Ding, X.Y. Zeng, Laser-induced breakdown spectroscopy in China, *Fronti. Phys.* 9 (4) (2014) 419–438.
- [3] H. Yin, Z. Hou, T. Yuan, Z. Wang, W. Ni, Z. Li, Application of spatial confinement for gas analysis using laser-induced breakdown spectroscopy to improve signal stability, *J. Anal. Atomic Spectrom.* 30 (4) (2015) 922–928.
- [4] P. Zhang, L. Sun, H. Yu, P. Zeng, L. Qi, Y. Xin, An image auxiliary method for quantitative analysis of laser-induced breakdown spectroscopy, *Anal. Chem.* 90 (7) (2018) 4686–4694.
- [5] T. Cvrtnickova, M.P. Mateo, A. Yañez, G. Nicolas, Laser Induced Breakdown Spectroscopy application for ash characterisation for a coal fired power plant, *Spectrochim. Acta B Atom Spectrosc.* 65 (8) (2010) 734–737.
- [6] X. Li, Z. Wang, S.L. Lui, Y. Fu, Z. Li, J. Liu, W. Ni, A partial least squares based spectrum normalization method for uncertainty reduction for laser-induced breakdown spectroscopy measurements, *Spectrochim. Acta B Atom Spectrosc.* 88 (2013) 180–185, 5.
- [7] J. Frydenvang, K.M. Kinch, S. Husted, M.B. Madsen, An optimized calibration procedure for determining elemental ratios using Laser-Induced Breakdown Spectroscopy, *Anal. Chem.* 85 (3) (2013) 1492–1500.
- [8] A. Matsumoto, A. Tamura, R. Koda, K. Fukami, Y.H. Ogata, N. Nishi, T. Sakka, On-site quantitative elemental analysis of metal ions in aqueous solutions by underwater laser-induced breakdown spectroscopy combined with electrodeposition under controlled potential, *Anal. Chem.* 87 (3) (2015) 1655–1661.
- [9] X. Li, Z. Wang, Y. Fu, Z. Li, W. Ni, A model combining spectrum standardization and dominant factor based partial least square method for carbon analysis in coal using laser-induced breakdown spectroscopy, *Spectrochim. Acta B Atom Spectrosc.* 99 (2014) 82–86.
- [10] A. Ciucci, M. Corsi, V. Palleschi, S. Rastelli, A. Salvetti, E. Tognoni, New procedure for quantitative elemental analysis by laser-induced plasma spectroscopy, *Appl. Spectrosc.* 53 (8) (1999) 960–964.
- [11] E. Tognoni, G. Cristoforetti, S. Legnaioli, V. Palleschi, A. Salvetti, M. Müller, I. Gornushkin, A numerical study of expected accuracy and precision in calibration-free laser-induced breakdown spectroscopy in the assumption of ideal analytical plasma, *Spectrochim. Acta B Atom Spectrosc.* 62 (12) (2007) 1287–1302.
- [12] V.N. Lednev, S.M. Pershin, Plasma stoichiometry correction method in laser-induced breakdown spectroscopy, *Laser Phys.* 18 (7) (2008) 850–854.
- [13] K.K. Herrera, E. Tognoni, N. Omenetto, B.W. Smith, J.D. Winefordner, Semi-quantitative analysis of metal alloys, brass and soil samples by calibration-free laser-induced breakdown spectroscopy: recent results and considerations, *J. Anal. Atomic Spectrom.* 24 (4) (2009) 413–425.
- [14] K.K. Herrera, E. Tognoni, I.B. Gornushkin, N. Omenetto, B.W. Smith, J.D. Winefordner, Comparative study of two standard-free approaches in laser-induced breakdown spectroscopy as applied to the quantitative analysis of aluminum alloy standards under vacuum conditions, *J. Anal. Atomic Spectrom.* 24 (4) (2009) 426–438.
- [15] L. Sun, H. Yu, Correction of self-absorption effect in calibration-free laser-induced breakdown spectroscopy by an internal reference method, *Talanta* 79 (2) (2009) 388–395.
- [16] D. Buljic, M. Corsi, G. Cristoforetti, S. Legnaioli, V. Palleschi, A. Salvetti, E. Tognoni, A procedure for correcting self-absorption in calibration free-laser induced breakdown spectroscopy, *Spectrochim. Acta B Atom Spectrosc.* 57 (2) (2002) 339–353.
- [17] M.V. Bel’Kov, V.S. Burakov, V.V. Kiris, N.M. Kozhukh, S.N. Raikov, Spectral standard-free laser microanalysis of gold alloys, *J. Appl. Spectrosc.* 72 (3) (2005) 376–381.
- [18] M. Corsi, G. Cristoforetti, V. Palleschi, A. Salvetti, E. Tognoni, A fast and accurate method for the determination of precious alloys caratage by laser induced plasma spectroscopy, *Eur. Phys. J. D At. Mol. Opt. Phys.* 13 (3) (2001) 373–377.
- [19] S.M. Pershin, F. Colao, V. Spizzichino, Quantitative analysis of bronze samples by laser-induced breakdown spectroscopy (LIBS): a new approach, model, and experiment, *Laser Phys.* 16 (3) (2006) 455–467.
- [20] L. Fornarini, F. Colao, R. Fantoni, V. Lazic, V. Spizzichino, Calibration analysis of bronze samples by nanosecond laser induced breakdown spectroscopy: a theoretical and experimental approach, *Spectrochim. Acta B Atom Spectrosc.* 60 (7–8) (2005) 1186–1201.
- [21] F. Colao, R. Fantoni, V. Lazic, L. Caneve, A. Giardini, V. Spizzichino, LIBS as a diagnostic tool during the laser cleaning of copper based alloys: experimental results, *J. Anal. Atomic Spectrom.* 19 (2004) 502–504.
- [22] J.A. Aguilera, C. Aragón, G. Cristoforetti, E. Tognoni, Application of calibration-free laser-induced breakdown spectroscopy to radially resolved spectra from a copper-based alloy laser-induced plasma, *Spectrochim. Acta B Atom Spectrosc.* 64 (7) (2009) 685–689.
- [23] V.S. Burakov, V.V. Kiris, P.A. Naumenkov, S.N. Raikov, Calibration-free laser spectral analysis of glasses and copper alloys, *J. Appl. Spectrosc.* 71 (5) (2004) 740–746.
- [24] I. Borgia, L.M. Burgio, M. Corsi, R. Fantoni, V. Palleschi, A. Salvetti, E. Tognoni, Self-calibrated quantitative elemental analysis by laser-induced plasma spectroscopy: application to pigment analysis, *J. Cult. Herit.* 1 (2000) S281–S286.
- [25] F. Colao, R. Fantoni, V. Lazic, A. Paolini, F. Fabbri, G.G. Ori, A. Baliva, Investigation of LIBS feasibility for in situ planetary exploration: an analysis on Martian rock analogues, *Planet. Space Sci.* 52 (1–3) (2004) 117–123.
- [26] L. Wang, C. Zhang, Y. Feng, Controlled calibration method for laser induced breakdown spectroscopy, *Chin. Opt. Lett.* 6 (1) (2008) 5–8.
- [27] B. Sallé, J.L. Lacour, P. Mauchien, P. Fichet, S. Maurice, G. Manhes, Comparative study of different methodologies for quantitative rock analysis by laser-induced breakdown spectroscopy in a simulated Martian atmosphere, *Spectrochim. Acta B Atom Spectrosc.* 61 (3) (2006) 301–313.
- [28] M. Boudhib, J. Hermann, C. Dutouquet, Compositional analysis of aerosols using calibration-free laser-induced breakdown spectroscopy, *Anal. Chem.* 88 (7) (2016) 4029–4035.
- [29] E. Tognoni, G. Cristoforetti, S. Legnaioli, V. Palleschi, Calibration-free laser-induced breakdown spectroscopy: state of the art, *Spectrochim. Acta B Atom Spectrosc.* 65 (1) (2010) 1–14.
- [30] S.A. Mansour, Self-absorption effects on electron temperature-measurements utilizing laser induced breakdown spectroscopy (LIBS)-Techniques, *Optic Photon. J.* 5 (03) (2015) 79.
- [31] C. Aragon, J. Bengoechea, J.A. Aguilera, Influence of the optical depth on spectral line emission from laser-induced plasmas, *Spectrochim. Acta B Atom Spectrosc.* 56 (6) (2001) 619–628.
- [32] B. Praher, V. Palleschi, R. Viskup, J. Heitz, J.D. Pedarnig, Calibration free laser-induced breakdown spectroscopy of oxide materials, *Spectrochim. Acta B Atom Spectrosc.* 65 (8) (2010) 671–679.
- [33] H. Fu, H. Wang, J. Jia, Z. Ni, F. Dong, Standard reference line combined with one-point calibration-free laser-induced breakdown spectroscopy (CF-LIBS) to quantitatively analyze stainless and heat resistant steel, *Appl. Spectrosc.* 72 (8) (2018) 1183–1188.
- [34] Takahashi T, Thornton B. Quantitative methods for compensation of matrix effects and self-absorption in Laser Induced Breakdown Spectroscopy signals of solids. *Spectrochim. Acta B Atom Spectrosc.* 138, 31–42.
- [35] J. Yang, C. Yi, . Xu, X. Ma, Laser-induced Breakdown spectroscopy quantitative analysis method via adaptive analytical line selection and relevance vector machine regression model, *Spectrochim. Acta B Atom Spectrosc.* 107 (2015) 45–55.
- [36] J. Dong, L. Liang, J. Wei, H. Tang, T. Zhang, X. Yang, H. Li, A method for improving the accuracy of calibration-free laser-induced breakdown spectroscopy (CF-LIBS) using determined plasma temperature by genetic algorithm (GA), *J. Anal. Atomic Spectrom.* 30 (6) (2015) 1336–1344.
- [37] A. Demidov, S. Eschlböck-Fuchs, A.Y. Kazakov, I.B. Gornushkin, P.J. Kolmhofer, J.D. Pedarnig, U. Panne, Monte Carlo standardless approach for laser induced breakdown spectroscopy based on massive parallel graphic processing unit computing, *Spectrochim. Acta B Atom Spectrosc.* 125 (2016) 97–102.
- [38] H.Y. Moon, K.K. Herrera, N. Omenetto, B.W. Smith, J.D. Winefordner, On the usefulness of a duplicating mirror to evaluate self-absorption effects in laser induced breakdown spectroscopy, *Spectrochim. Acta B Atom Spectrosc.* 64 (7) (2009) 702–713.
- [39] Z. Zhu, J. Li, Y. Guo, X. Cheng, Y. Tang, L. Guo, X. Zeng, Accuracy improvement of boron by molecular emission with a genetic algorithm and partial least squares regression model in laser-induced breakdown spectroscopy, *J. Anal. Atomic Spectrom.* 33 (2) (2017).
- [40] N. Konjević, Plasma broadening and shifting of non-hydrogenic spectral lines: present status and applications, *Phys. Rep.* 316 (6) (1999) 339–401.
- [41] C. Aragón, J.A. Aguilera, CSigma graphs: a new approach for plasma characterization in laser-induced breakdown spectroscopy, *J. Quant. Spectrosc. Radiat. Transf.* 149 (2014) 90–102.
- [42] J. Hermann, D. Grojo, E. Axente, V. Craciun, Local thermodynamic equilibrium in a laser-induced plasma evidenced by blackbody radiateon, *Spectrochim. Acta Part B At. Spectrosc.* 144 (2018) 82–86.
- [43] T. Li, S. Sheta, Z. Hou, J. Dong, Z. Wang, Impacts of a collection system on laser-induced breakdown spectroscopy signal detection, *Appl. Opt.* 57 (21) (2018) 6120–6127.
- [44] M. Morháč, V. Matoušek, Complete positive deconvolution of spectrometric data, *Digit. Signal Process.* 19 (3) (2009) 372–392.

- [45] Z. Wang, J. Feng, L. Li, W. Ni, Z. Li, A multivariate model based on dominant factor for laser-induced breakdown spectroscopy measurements, *J. Anal. Atomic Spectrom.* 26 (2011) 2289–2299.
- [46] Z. Wang, J. Feng, L. Li, W. Ni, Z. Li, A non-linearized PLS model based on multivariate dominant factor for laser-induced breakdown spectroscopy measurements, *J. Anal. Atomic Spectrom.* 26 (2011) 2175–2182.
- [47] J. Feng, Z. Wang, L. West, Z. Li, W. Ni, A PLS model based on dominant factor for coal analysis using laser-induced breakdown spectroscopy, *Anal. Bioanal. Chem.* 400 (2011) 3261–3271.